

## Liquid-gas phase transition in hot nuclei studied with INDRA

B. Borderie<sup>a</sup>, R. Bougault<sup>b</sup>, P. Désesquelles<sup>a</sup>, E. Galichet<sup>a</sup>, B. Guiot<sup>c \*</sup>, Ph. Lantesse<sup>d</sup>, N. Le Neindre<sup>a</sup>, J. Marie<sup>b</sup>, M. Pârlog<sup>e</sup>, M. Pichon<sup>b</sup>, M. F. Rivet<sup>a</sup>, E. Rosato<sup>f</sup>, G. Tăbăcaru<sup>e †</sup>, M. Vigilante<sup>f</sup> and J. P. Wieleczko<sup>c</sup>

<sup>a</sup>Institut de Physique Nucléaire, IN2P3-CNRS, F-91406 Orsay Cedex, France

<sup>b</sup>LPC Caen, IN2P3-CNRS/ENSICAEN et Université, F-14050 Caen cedex, France

<sup>c</sup>GANIL, DSM-CEA/IN2P3-CNRS, B.P. 5027, F-14021 Caen Cedex, France

<sup>d</sup>Institut de Physique Nucléaire, IN2P3-CNRS et Université, Villeurbanne, France

<sup>e</sup> National Institute for Physics and Nuclear Engineering, Bucharest-Măgurele, Romania

<sup>f</sup>Dipartimento di Scienze Fisiche e Sezione INFN, Università di Napoli, Napoli, Italy

Thanks to the high detection quality of the INDRA array, signatures related to the dynamics (spinodal decomposition) and thermodynamics (negative microcanonical heat capacity) of a liquid-gas phase transition have been simultaneously studied in multifragmentation events in the Fermi energy domain. The correlation between both types of signals strongly supports the existence of a first order phase transition for hot nuclei.

### 1. Introduction

The main goal of multifragmentation studies concerns its relation with subcritical and/or critical phenomena. Thus it is fully connected to the nature of the phase transition of nuclear matter which is expected of the liquid-gas type due to the specific form of the nucleon-nucleon interaction. Despite the large number of experimental results, fundamental questions could not be addressed for a long time. We are facing an exciting but also very complex subject where only very sophisticated detector arrays like INDRA [ 1, 2] can produce the high quality experiments needed [ 3, 4, 5, 6, 7, 8, 9, 10, 11]. From collisions between nuclei we hope to reveal a phase transition for those finite objects and derive the related equation of state of nuclear matter. In parallel to the experimental effort a big theoretical effort started a few years ago to characterize and propose signatures of phase transitions in finite systems [ 12, 13, 14]. Phase transitions should be reconsidered from a more general point of view, out of the thermodynamical limit. Thus, experiments on nuclear multifragmentation are also used as test-bench for the elaboration of the statistical physics of finite systems.

---

\*Present address: INFN, Sezione di Bologna and Dipartimento di Fisica, Università di Bologna, Italy

†Present address: Cyclotron Institute, Texas A&M University, College Station, Texas 77845, USA

The paper describes some major recent results obtained with the INDRA array. It is organized as follows. After some information concerning the description of collisions and associated simulations, the dynamics of phase transition in hot nuclei and the related proposed signature will be presented. Then specific phase transition signals related to the thermodynamics of finite systems will be discussed in terms of robustness. Finally, from systematic studies, the coherence between signals will be demonstrated.

## 2. Description of collisions and multifragmentation

Semi-classical simulations of nucleus-nucleus collisions based on the nuclear Boltzmann equation (VUU, LV, BUU, BNV) [ 15, 16, 17, 18], were very successful in reproducing a variety of experimental dynamical observables. However as they follow the time evolution of the one body density, considering only the average effect of collisions between particles (two-body collisions), they ignore fluctuations about the main trajectory of the system (deterministic description), which becomes a severe drawback if one wants to describe processes involving instabilities, bifurcations or chaos. Such approaches are appropriate during the early stages of nuclear collisions, when the system is hot and compressed, but they become inadequate when expansion and cooling have brought the system in the instability (spinodal) zone of the phase diagram. In such a scenario, it is essential to include the fluctuations. This is done in Quantum Molecular Dynamics methods and in the Stochastic Mean Field (SMF) approach. We shall now focus on SMF approach, a natural evolution of deterministic semi-classical simulations, which was compared to INDRA data.

### 2.1. Brownian one-body dynamics (BOB)

In BOB simulations, fluctuations in one-body dynamics are introduced by employing a Brownian force in the kinetic equations. The starting point is the so-called Boltzmann-Langevin equation (BLE):

$$\frac{\partial f}{\partial t} = \{h[f], f\} + \bar{I}[f] + \delta I[f] \quad (1)$$

which was introduced for heavy-ion collisions in references [ 19, 20].  $f$  is the one-body phase space density. The first term on the r.h.s. produces the collisionless propagation of  $f$  in the self-consistent one-body field described by the effective Hamiltonian. The second term (second source of evolution called collision term) represents the average effect of the residual Pauli-suppressed two-body collisions; this is the term included in LV, BUU and BNV simulations. The third term is the Langevin term which accounts for the fluctuating part of the two-body collisions. Exact numerical solutions of the BLE are very difficult to obtain and have only be calculated for schematic cases in one or two dimensions [ 21]. Therefore various approximate treatments of the BLE have been developed. The basic idea of BOB [ 22] is to replace the fluctuating term by

$$\delta \tilde{I}[f] = -\delta \mathbf{F}[f] \cdot \frac{\partial f}{\partial \mathbf{p}} \quad (2)$$

where  $\delta \mathbf{F}(\mathbf{r}, t)$  is the associated Brownian force ( $\langle \delta \mathbf{F} \rangle = 0$ ). Since the resulting Brownian one-body dynamics mimics the BL evolution, the stochastic force is assumed to be

local in space and time. The strength of the force is adjusted to reproduce the growth of the most unstable modes for infinite nuclear matter in the unstable spinodal region (see next section).

## 2.2. Comparison with data

The comparison was made for two very heavy fused systems produced in Xe+Sn and Gd+U central collisions which undergo multifragmentation with the same available excitation energy ( $\sim 7$  MeV per nucleon). Stochastic mean-field simulations were performed for head-on collisions, thus neglecting shape effects. Ingredients of simulations are detailed in [23]. After BOB simulation a second step, starting from the phase space configuration of the primary fragments as given by BOB, followed the fragment statistical deexcitation while preserving space-time correlations. Finally the events were filtered to account for the experimental device. These complete simulations very well reproduce the observed multiplicity and charge distributions of fragments [23]. Particularly the independence of the charge distribution against the mass of the system experimentally observed is recovered [24]. More detailed comparisons also show a good agreement [23, 25]. Kinetic properties of fragments are rather well accounted for especially for the Gd+U system. For Xe+Sn, the calculated energies fall  $\sim 20\%$  below the measured values which remains satisfactory if one remembers that there were no adjustable parameters in the simulation.

## 2.3. What have we learnt ?

From the good agreement between dynamical simulations and data a complete scenario is proposed [23]. After a gentle compression ( $\sim 1.25\rho_0$ ), maximum at 40 fm/c, systems expand and enter the unstable (negative compressibility) spinodal region at around 80 fm/c. Slightly later ( $\sim 100$  fm/c) thermal equilibrium is achieved ( $\langle T \rangle = 4$  MeV) at low density ( $\sim 0.4\rho_0$ ) and systems have lost  $\sim 5\%$  of their initial masses by emitting preequilibrium particles. The radial velocities at the surface ( $\sim 0.1c$ ) reveal the expansion of the systems and density fluctuations (spinodal instabilities) have time to develop leading to the formation of fragments. Around 250 fm/c after the beginning of collisions the fragments do not interact any more, they are in thermal equilibrium and still bear an average excitation energy of  $\sim 3$  MeV per nucleon: it is the freeze-out time with the associated freeze-out volume, it corresponds to the end of these BOB simulations.

## 3. Dynamics of the phase transition and related signal

Thermodynamics describes phase transitions in terms of “static conditions”. Information on existence and coexistence of phases are derived depending on thermodynamical parameters (temperature, pressure, ...). How to pass from a phase to another ? What is the time needed ? To answer these questions, dynamics of phase transitions must be studied. A phase transition is a dynamical phenomenon with its proper kinetics. The aim of this section is to discuss the dynamics of the phase transition which can be involved in hot unstable nuclei. Two mechanisms are candidates. (i) Nucleation which is associated with a transport of matter; diffusion is the key mechanism which controls the kinetics; we are in presence of heterogeneous fluctuations. (ii) Spinodal decomposition which occurs when a system spontaneously develops local fluctuations of concentration or density which grow exponentially with time; characteristic time is related to the most unstable

modes. In contrast with nucleation, we are here dealing with homogeneous fluctuations. Given the agreement discussed in the previous section, we will now focus on spinodal decomposition.

### 3.1. Spinodal decomposition: from nuclear matter to nuclei

In the spinodal region some modes are amplified because of the instability. Their associated characteristic times are almost identical, around 30- 50 fm/c, depending on density ( $\rho_0/2$ - $\rho_0/8$ ) and temperature (0-9MeV) [ 26, 27]. Within this scenario a breakup into nearly equal-sized “primitive” fragments should be favoured in relation to the wavelengths of the most unstable modes [ 28]. However this simple picture is predicted to be strongly blurred by several effects: beating of different modes, coalescence of nascent fragments, secondary decay of excited fragments and, above all, finite size effects [ 29]. Therefore only a weak proportion of multifragmentation events with nearly equal-sized fragments is expected.

### 3.2. The related fossil signal: enhanced production of nearly equal-sized fragments

A few years ago a new method called higher order charge correlations [ 30], which has been recently improved [ 31], was proposed to enlighten any extra production of events with specific fragment partitions. The high sensitivity of the method makes it particularly appropriate to look for small numbers of events as those expected to have kept a memory of spinodal decomposition properties. Thus, such a charge correlation method allows to examine model independent signatures that would indicate a preferred decay into a number of equal-sized fragments in events from experimental data or from simulations. All fragments ( $Z \geq 5$ ) of one event with fragment multiplicity  $M = \sum_Z n_Z$ , where  $n_Z$  is the number of fragments with charge  $Z$  in the partition, are taken into account. By means of the normalized first and second order moments of the fragment charge distribution in the event:

$$\langle Z \rangle = \frac{1}{M} \sum_Z n_Z Z, \quad \sigma_Z^2 = \frac{1}{M} \sum_Z n_Z (Z - \langle Z \rangle)^2 \quad (3)$$

one may define the higher order charge correlation function:

$$1 + R(\sigma_Z, \langle Z \rangle) = \frac{Y(\sigma_Z, \langle Z \rangle)}{Y'(\sigma_Z, \langle Z \rangle)} \Big|_M \quad (4)$$

Here, the numerator  $Y(\sigma_Z, \langle Z \rangle)$  is the yield of events with given  $\langle Z \rangle$  and  $\sigma_Z$  values and the evaluation of the denominator (uncorrelated yield) is deduced from the exact multinomial formula under total charge conservation constraint (see ref. [ 31, 32] for details).

We shall now discuss the results obtained for fused systems produced in  $^{129}\text{Xe}$  central collisions on  $^{nat}\text{Sn}$  at four incident energies (32, 39, 45 and 50 AMeV) [ 32]. At 32 AMeV the present analysis fully confirms the previous one obtained with the original method [ 33] and the extra-percentage of events with nearly equal-sized fragments is maximum at 39 AMeV incident energy. The excitation function is displayed in fig. 1. Information on the associated thermal excitation energies (and extra radial collective energy) involved over the incident energy domain studied can be provided by the SMM model [ 34] which well describes static and dynamic observables of fragments. Starting from a freeze-out

volume fixed at three times the normal volume, the thermal excitation energies of the dilute and homogeneous system, extracted from SMM, vary from 5.0 to 7.0 AMeV and the added radial expansion energy remains low: from 0.5 to 2.2 AMeV [ 35, 36]. A rise and fall of the percentage of “fossil partitions” from spinodal decomposition is measured. Results from BOB simulations ( head-on  $^{129}\text{Xe}$  on  $^{119}\text{Sn}$  collisions at 32 AMeV) are also shown; although all events in the simulation arise from spinodal decomposition, only a very small fraction of the final partitions ( $\sim 1\%$ ) have kept nearly equal-sized fragments. Mainly due to finite size effects the signature of spinodal decomposition can only reveal itself as a weak “fossil” signal.

As a conclusion of that section we can say that, supported by theoretical simulations, we interpret our data as a signature of spinodal instabilities as the origin of multifragmentation of those fused systems in the Fermi energy domain. Spinodal decomposition describes the dynamics of a first order phase transition, the present observations thus support the existence of such a transition for hot finite nuclear matter.

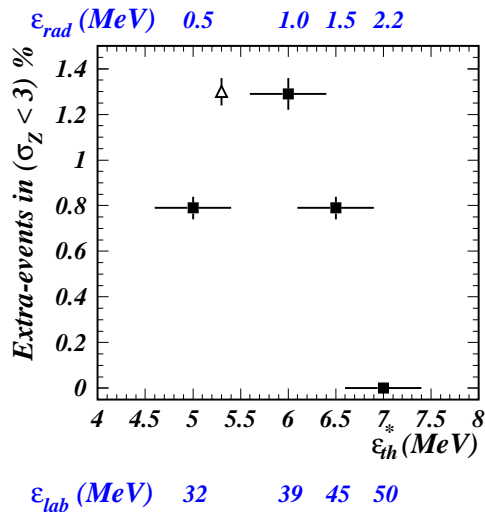


Figure 1. Abnormal production of events with nearly equal-sized fragments ( $\sigma_Z < 3$  corresponds to the upper limit of the islet of peaks - see [ 32] for details) as a function of thermal excitation energy (deduced from SMM): full points. The incident and radial energy scales are also indicated. The open point refers to the result from BOB simulations; the average thermal energy is used.

#### 4. Thermodynamics of finite systems and related signals

In section 2 we have shown that experimental charge and multiplicity distributions were reproduced with BOB simulations while average fragment kinetic energies were accounted for within 20 %. These same data were also well accounted for with the statistical model SMM [ 35, 36, 37]. From these two findings we can deduce that the dynamics involved is sufficiently chaotic to finally explore enough of the phase space in order to describe fragment production through a statistical approach. Selected events correspond to “statistical samples” (which have nothing to do with ergodic arguments) and therefore we can go further and use statistical mechanics of finite systems.

#### 4.1. Different signals and their robustness

From statistical physics of finite systems three direct signals of a first order phase transition are proposed: (i) the caloric curve at constant pressure, which is predicted to present a negative curvature, (ii) the presence of negative microcanonical heat capacity [13] and (iii) the existence of a bimodality of the event distribution as a function of an order parameter [38]. They are all related to a curvature anomaly of a thermodynamical potential due to surface effects in the unstable region of coexistence.

Do those signals have equivalent robustness? Experimentally one does not explore the caloric curves at constant pressure nor at constant volume. In fact many different measured caloric curves can be generated from experiments depending on the path followed on the microcanonical equation of state surface (T versus excitation energy and average volume). Therefore signals from shapes of caloric curves (plateau-like) appear not as robust as the two others signals. The method proposed to measure the microcanonical heat capacity uses partial energy fluctuations. Abnormal large fluctuations (as compared to the canonical expectation) are predicted to be always seen, independently of the path, if microcanonical negative heat capacity is present [39]. Finally bimodality is predicted to be very robust.

#### 4.2. Abnormal kinetic energy fluctuations and negative microcanonical heat capacity

The prescription proposed to estimate microcanonical heat capacity is based on the fact that for a given total energy of a system, the average partial energy stored in a part of the system is a good microcanonical thermometer, while the associated fluctuations can be used to construct the heat capacity [13]. From experiments the most simple decomposition of the total energy  $E^*$  is in a kinetic part  $E_1$  and a potential part  $E_2$  (Coulomb energy + total mass excess). However these quantities have to be determined at freeze-out and consequently it is necessary to trace back this configuration on an event by event basis. This needs, in principle, the knowledge of the freeze-out volume and of all the particles evaporated from primary hot fragments including the undetected neutrons. Consequently some reasonable working hypotheses are used, eventually constrained by specific experimental results [8]. An example of results obtained from INDRA data is displayed in fig. 2.

### 5. Observation of correlated signals

The spinodal region is also thermally unstable. This property has a well known consequence at the thermodynamical limit: the condition of maximal entropy (Maxwell construction) fixes a constant temperature for a given isobar in the coexistence region. But for finite systems the entropy presents a convex dip in that region and a direct consequence is the occurrence of a negative heat capacity. Thus, when spinodal decomposition is observed, one must measure a negative heat capacity. The reverse is not true because spinodal decomposition needs sufficient time to occur (about 100 fm/c, see subsection 3.1). Thus, systems may penetrate the spinodal region and multifragment through nucleation rather than spinodal decomposition.

Therefore both signals (spinodal decomposition and negative microcanonical heat capacity) have been simultaneously studied on different fused systems which undergo mul-

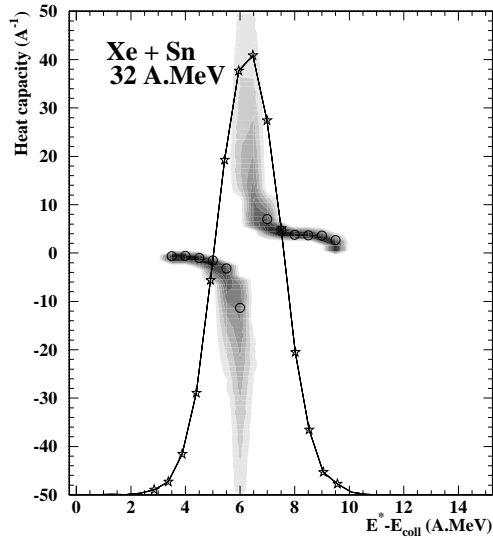


Figure 2. Microcanonical heat capacity per nucleon as a function of the excitation energy (corrected in average for the radial collective energy) measured in central collisions between Xe and Sn. From [ 40]

tifragmentation [ 36, 32, 41]. Results are summarized in table1. For the different systems

Table 1

Summary of the findings for phase transition signals.

system	Ni+Au	Ni+Ni	Xe+Sn	Xe+Sn	Ni+Au	Xe+Sn	Xe+Sn
Incident Energy AMeV	32.	32.	32.	39.	52.	45.	50.
Thermal energy AMeV	$5.0 \pm 1.0$	$5.0 \pm 1.0$	$5.0 \pm 0.5$	$6.0 \pm 0.5$	$6.0 \pm 1.0$	$6.5 \pm 0.5$	$7.0 \pm 0.5$
Radial energy AMeV	0.	$0.8 \pm 0.5$	$0.5 \pm 0.2$	$1.0 \pm 0.3$	0.	$1.5 \pm 0.4$	$2.2 \pm 0.4$
Spinodal decomposition	no	yes?	yes	yes	yes	yes	no
Negative microc. heat capacity	no	yes	yes	yes	yes	yes?	no

we have also indicated the associated thermal and radial collective energies extracted (see subsection 3.2. and reference [ 41] for details). We observe a correlation between the two signals, which strongly supports the presence of a first order phase transition for hot nuclei undergoing multifragmentation in the Fermi energy domain. Moreover this correlation reinforces the fact that spinodal decomposition (even if evidenced by a small fossil signal) is indeed the dynamics of the phase transition. Both signals are present when a total (thermal+radial) energy in the range 5.5-7.0 AMeV is measured. Note that the effect of a very gentle compression phase leading to 0.5-1.0 AMeV radial expansion energy plays the same role as a slightly higher thermal energy (Ni+Au system at 52 AMeV). This can be understood in terms of a required threshold for expansion energy; in the latter case this threshold should be reached by thermal expansion only.

## 6. Other signals

Several other signals are under studies using INDRA data. The so called Fisher scaling is observed on a large set of central (fused systems) and peripheral collisions [ 42]. It was tentatively used in reference [ 11] to derive information on the critical point of finite neutral nuclear matter; we notice that, for the fused systems previously discussed, the observed “pseudo” critical point appears inside the coexistence zone (presence of the two correlated signals discussed in the previous section). This last remark is also valid for analysis of data within the universal fluctuations framework (see [ 43] - fluctuations of the size of the heaviest fragment). Within this theory, transition from an ordered phase to a disordered phase can be well identified through the largest fluctuations nature provides for an order parameter. Finally one can make the more general comment that for finite nuclei the largest fluctuations measured (kinetic energy and size of the heaviest fragment) are associated to the coexistence region (see also [ 14]).

Concerning bimodality, encouraging results have been recently obtained using data from peripheral Au+Au collisions studied with INDRA at GSI [ 44]. A correlation between bimodality and negative microcanonical heat capacity is observed.

## 7. Conclusions and perspectives

The correlation observed between the presented signals completely argues for the existence of a liquid-gas type phase transition in hot nuclei. The nature of the dynamics of the phase transition has been evidenced; spinodal instabilities are thus shown for the first time in a finite system. Many systematic studies including correlations between different signals, independent measurements to characterize systems at freeze-out, are now required for establishing a metrology of the phase diagram and the related equation of state for hot nuclei and nuclear matter. The introduction of the N/Z degree of freedom appears also for the future as a second very exciting challenge.

## REFERENCES

1. J. Pouthas et al., Nucl. Instr. and Meth. in Phys. Res. A 357 (1995) 418.
2. J. Pouthas et al., Nucl. Instr. and Meth. in Phys. Res. A 369 (1996) 222.
3. M. D’Agostino et al., Phys. Lett. B 473 (2000) 219.
4. J. A. Hauger et al. (EOS collaboration), Phys. Rev. C 62 (2000) 024616.
5. J. B. Elliott et al. (EOS collaboration), Phys. Rev. C 62 (2000) 064603.
6. H. Xu et al., Phys. Rev. Lett. 85 (2000) 716.
7. B. Borderie, J. Phys. G: Nucl. Part. Phys. 28 (2002) R217 and references therein.
8. M. D’Agostino et al., Nucl. Phys. A 699 (2002) 795.
9. A. H. Raduta et al., Phys. Rev. C 65 (2002) 054610.
10. M. Kleine Berkenbusch et al., Phys. Rev. Lett. 88 (2002) 022701.
11. J. B. Elliott et al., Phys. Rev. Lett. 88 (2002) 042701.
12. D. H. E. Gross, Microcanonical Thermodynamics - Phase Transitions in “small” systems, World Scientific, Singapore, 2001.
13. P. Chomaz et al., T. Dauxois et al. (eds.) Dynamics and Thermodynamics of systems



with long range interactions, Springer-Verlag, Heidelberg, 2002, vol. 602 of Lecture Notes in Physics, 68–129.

14. F. Gulminelli, LPCC 03-06 (2003) and references therein.
15. H. Kruse et al., Phys. Rev. C 31 (1985) 1770.
16. C. Grégoire et al., Nucl. Phys. A 465 (1987) 317.
17. G. F. Bertsch et al., Phys. Rep. 160 (1988) 189.
18. A. Bonasera et al., Phys. Rep. 243 (1994) 1.
19. S. Ayik et al., Phys. Lett. B 212 (1988) 269.
20. J. Randrup et al., Nucl. Phys. A 514 (1990) 339.
21. P. Chomaz et al., Phys. Lett. B 254 (1991) 340.
22. P. Chomaz et al., Phys. Rev. Lett. 73 (1994) 3512.
23. J. D. Frankland et al. (INDRA collaboration), Nucl. Phys. A 689 (2001) 940.
24. M. F. Rivet et al. (INDRA collaboration), Phys. Lett. B 430 (1998) 217.
25. G. Tăbăcaru et al. (INDRA collaboration), G. Bonsignori et al. (eds.) Proc. of the International Conference on Structure of the Nucleus at the Dawn of the Century, Bologna, Italy, World Scientific, 2001, Vol. 1, Nucleus-Nucleus collisions, 321.
26. M. Colonna et al., Nucl. Phys. A 613 (1997) 165.
27. D. Idier et al., Ann. Phys. Fr. 19 (1994) 159.
28. S. Ayik et al., Phys. Lett. B 353 (1995) 417.
29. B. Jacquot et al., Phys. Lett. B 383 (1996) 247.
30. L. G. Moretto et al., Phys. Rev. Lett. 77 (1996) 2634.
31. P. Désesquelles, Phys. Rev. C 65 (2002) 034604.
32. G. Tăbăcaru et al., Eur. Phys. J. A 18 (2003) in press, nucl-ex/0212018.
33. B. Borderie et al. (INDRA collaboration), Phys. Rev. Lett. 86 (2001) 3252.
34. J. Bondorf et al., Phys. Rep. 257 (1995) 133.
35. S. Salou, thèse de doctorat, Université de Caen (1997), GANIL T 97 06.
36. N. Le Neindre, thèse de doctorat, Université de Caen (1999), LPCC T 99 02.
37. N. Le Neindre et al. (INDRA collaboration), G. Bonsignori et al. (eds.) Proc. of the International Conference on Structure of the Nucleus at the Dawn of the Century, Bologna, Italy, World Scientific, 2001, Vol. 1, Nucleus-Nucleus collisions, 221.
38. P. Chomaz et al., Phys. Rev. E 64 (2001) 046114.
39. P. Chomaz et al., Phys. Rev. Lett. 85 (2000) 3587.
40. N. Le Neindre et al. (INDRA collaboration), I. Iori et al. (eds.) Proc. XXXVIII Int. Winter Meeting on Nuclear Physics, Bormio, Italy, Ricerca scientifica ed educazione permanente, 2000, 404.
41. B. Guiot, thèse de doctorat, Université de Caen (2002), GANIL T 02 04.
42. N. Le Neindre et al. (INDRA collaboration), I. Iori et al. (eds.) Proc. XL Int. Winter Meeting on Nuclear Physics, Bormio, Italy, Ricerca scientifica ed educazione permanente, 2002, 144.
43. R. Botet et al., Phys. Rev. Lett. 86 (2001) 3514.
44. M. Pichon et al. (INDRA and ALADIN collaborations), I. Iori et al. (eds.) Proc. XLI Int. Winter Meeting on Nuclear Physics, Bormio, Italy, Ricerca scientifica ed educazione permanente, 2003, 149.